



Charge transport and Hall effect in rubrene single-crystal transistors under high pressure

Y. Okada,^{1,2} K. Sakai,¹ T. Uemura,¹ Y. Nakazawa,² and J. Takeya^{1,*}

¹*ISIR, Osaka University, Ibaraki 567-0047, Japan*

²*Graduate School of Science, Osaka University, Toyonaka 560-0043, Japan*

(Received 25 October 2011; revised manuscript received 25 November 2011; published 14 December 2011)

Four-terminal conductivity and Hall coefficient are measured in high-mobility rubrene single-crystal field-effect transistors as functions of gate electric field and external hydrostatic pressure up to 900 MPa. Estimating charge density directly from the measured Hall coefficient regardless of contraction in the gate dielectric layer, genuine pressure dependence of the mobility is extracted. It turned out that enhanced intermolecular charge transfer causes an increase in the mobility of the bandlike charge carriers by 20% GPa up to 600 MPa, which is typically one order of magnitude larger than that in inorganic semiconductors. We also found negative pressure coefficient for the mobility above 600 MPa, suggesting that the external hydrostatic force causes additional molecular displacement due to a specific molecular shape.

DOI: [10.1103/PhysRevB.84.245308](https://doi.org/10.1103/PhysRevB.84.245308)

PACS number(s): 73.61.Ph, 72.80.Le, 73.40.-c

I. INTRODUCTION

Organic semiconductor solids are attracting considerable attention based on their charge transport controlled by field effect, applicability of simple printing production processes, and mechanical flexibility, in prospect of establishing plastic and printed electronics industry. Since such solids are assemblies of van der Waals bonded π -conjugated molecules, macroscopic transport is composed of nanoscale intermolecular charge transfer of π -electronic carriers, which necessarily results in its sensitivity to molecular arrangement. Here, we introduce a method of measuring the effect of hydrostatic pressure on the conductivity in organic semiconductor crystals inducing high-mobility charge with the application of electric field at the semiconductor surfaces.

It has been established for some high-mobility organic semiconductors with the structure of field-effect transistors (FET) that bandlike transport is realized for the surface charge with relatively low carrier density less than 10^{12} cm^{-2} , artificially introduced in an intrinsic semiconductor composed of a single molecular species.¹⁻³ The mobility in such organic single-crystal FETs already exceeds $10 \text{ cm}^2/\text{V s}$ in several compounds.⁴⁻⁸ In addition to the measurement of common transfer characteristics of drain current I_D as a function of gate voltage V_G shown in former pioneering studies,^{9,10} we perform four-terminal conductivity measurement to exclude extrinsic influence of the metal/semiconductor contact resistance. Moreover, we measured Hall coefficient simultaneously to deduce the correct pressure coefficient estimating the change in dielectric capacitance and thickness of the gate dielectric insulators, providing a route to study the so-called “structure-property” relation.

The size of thus deduced pressure dependence of mobility turned out to be much smaller than previously reported results in the pressure region below 600 MPa but is still about seven times larger than in the typical experiments reported for silicon and other inorganic semiconductors.⁹⁻¹¹ Interestingly, the mobility starts to decrease with further increasing pressure above 600 MPa. Noting that the organic solids are composed of molecules with peculiar shape, the application of pressure not only diminishes distance between centers of adjacent molecules but relative positions of equivalent atoms in the

two molecules. It is speculated that the anomalous negative pressure effect can be caused by such additional degrees of freedom in molecular solids.

II. EXPERIMENT

Figure 1(a) illustrates a schematic view of the samples used for the measurement. We use rubrene for the semiconductor material, as it is the best studied compound for organic single crystal transistors.¹²⁻¹⁴ The method of laminating crystals on gate-insulator substrate is employed to fabricate the field-effect transistor (FET) devices, in which carrier mobility exceeding $10 \text{ cm}^2/\text{V s}$ has been achieved.⁶ We have already established techniques of low-temperature and Hall-effect measurements in ambient atmosphere^{3,15} so that the method of pressurized measurement was ready to be developed by manufacturing pressure cells.

Rubrene single crystals are grown from gas phase by physical vapor transport.¹⁶ A commercial sublimed grade product of Aldrich 551112 was used for the starting material. The raw materials are vaporized at 295°C and coarse-crystallized at 240°C in a two-zone tube furnace in a stream of Ar gas. The resultant coarse crystals were brought to the sublimation boat and were revaporized so that purified rubrene crystals can be grown.

We use polyethylene naphthalate (PEN) for the substrate because of its similar restriction coefficient to most organic semiconductors in order not to damage the devices under pressure. We note that substrates made of silicon broke the rubrene crystals into pieces when pressurized. A gate electrode of 30-nm gold film is first vacuum deposited with a rectangular shape that is identical to the semiconductor channel. A gate-insulating layer of CYTOP (Asahi Glass Co.) is coated and cured at 110°C for 2h. The typical thickness of the CYTOP film is about $1 \mu\text{m}$ and its dielectric constant is known to be 2.0 with the unit of that of vacuum. Source, drain, and four additional voltage-monitoring pads are formed with vacuum deposited gold through a shadow metal mask so that a gate electrode is placed inside the surrounding pads. A flakelike rubrene single crystal with a thickness of less than $1 \mu\text{m}$ is carefully taken and is laminated to attach all the prepared

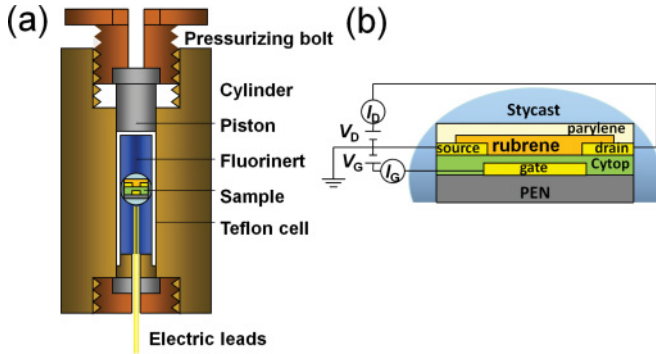


FIG. 1. (Color online) Schematic illustrations of (a) the high-pressure cell used for the present measurement and (b) the diagram to measure the transport of rubrene single-crystal field-effect transistors.

six gold pads on the substrates. Finally, the Hall-bar-shaped channel is fabricated with the use of laser etching equipment so that the central channel is on the gate electrode. Such adjustment is helpful to minimize the gate-leakage current. The channel length and width are 150 and 50 μm , respectively. The distance l between the voltage-probing pads in the direction of the channel length is 50 μm . The device is encapsulated with a few- μm parylene and then completely filled in epoxy (STYCAST 1266). The whole piece is placed in a standard Cu-Be pressure cell and Fluorinert FC70/77 is used for the pressurizing media.

As illustrated in Fig. 1(b), voltages V_1 , V_2 , and V_3 are measured at three different positions in the channel, so that four-terminal (sheet) conductivity $\sigma_{\square} [=I_D/(V_2 - V_1)l/W]$ and transverse voltage ($V_3 - V_1$) are measured simultaneously as a function of gate voltage V_G . σ_{\square} equals the product of mobility μ and charge density Q . Therefore μ is defined on the four-terminal measurement

$$\mu = 1/C \cdot \partial\sigma/\partial V_G, \quad (1)$$

where C denotes the capacitance of the CYTOP gate insulator in a unit area. We note that C actually depends on the applied pressure P , so that the profile of $C(P)$ should be known to deduce correct values of μ for the pressurized rubrene single-crystal FETs. The Hall-effect experiments are useful for this purpose, measuring the carrier density directly as a function of V_G .

For the Hall-effect measurement, magnetic field is swept back and forth at least three times in the range -10 – 10 T, so that the slowly drifting signal is subtracted to evaluate ΔV_H for the peak-to-peak magnetic field and R_H is evaluated by $\Delta V_H/(I\Delta B)$, where $\Delta B = 20$ T. It is known that $1/R_H$ equals Q as long as the charge is mobile following the free-electron-like band-transport mechanism. Recently, it has been shown that carriers induced in the FETs of such high-mobility organic semiconductors as rubrene, DNNT, alkyl-DNNT, a pentacene derivative [1,4,8,11-tetramethyl-6,13-triethylsilyl ethynyl pentacene (TMTES-P)] fulfill this requirement.^{1–3,7,15,17} Therefore Q can be estimated independently without using values of C , when R_H is measured for the band-transport systems by performing the Hall-effect experiment.

III. RESULTS AND DISCUSSION

A. Hall effect

Figure 2(a) shows the plot of the inverse Hall coefficient as a function of gate voltage for a rubrene single-crystal device at room temperature. At an ambient pressure, $1/R_H$ increases with negative V_G in accordance with the free-electron formula $1/R_H = |C_0 V_G|$ within the accuracy of the measurement with the use of the gate dielectric capacitance C_0 at 1 atm, presenting a clear indication of the diffusive band transport. The four-terminal sheet conductivity is plotted together, showing a monotonic evolution of σ_{\square} with negative V_G due to the hole accumulation. μ is estimated to be approximately 18.2 $\text{cm}^2/\text{V s}$ using Eq. (1).

Given that the charge in rubrene single crystals propagates as band-transport carriers and that $1/R_H$ equals Q even under pressure, $C(P)$ is estimated by the slope in Fig. 1(a). The plot shown in Fig. 2(b) indicates that C changes as

$$C(P)/C_0 = 1 + 0.00021P \quad (2)$$

within the linear approximation. The result is consistent to the idea that capacitance increases as the result of diminishing

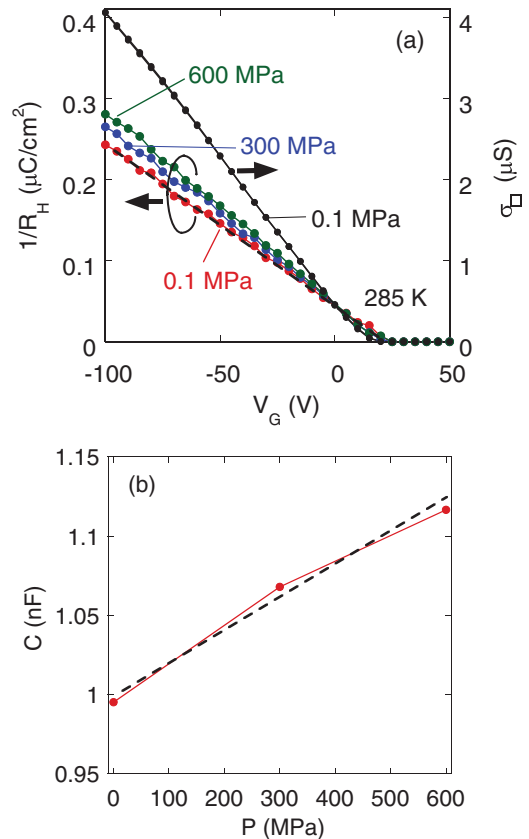


FIG. 2. (Color online) (a) Inverse Hall coefficient under hydrostatic pressures of 0.1, 300, and 600 MPa as a function of gate voltage for a rubrene single-crystal transistor at 285 K. Black dashed line indicates charge carrier density estimated from the gate dielectric capacitance. Evolution of sheet conductivity with the application of gate voltages is plotted together for 0.1 MPa. (b) Gate dielectric capacitance as a function of applied hydrostatic pressure. The dashed line indicates the result of linear fit.

d ; though there may be pressure dependence in the dielectric constant, this effect is also included in Eq. (2). Moreover, since the pressure dependence is almost the same down to 200 K as the result of the Hall-effect measurement performed at lower temperatures, we apply the same formula for the data in the temperature range down to 200 K.

B. Pressure-dependent mobility

Figure 3(a) shows transfer characteristics for the four-terminal conductivity at room temperature measured under various pressures. The residual conductivity at $V_G = 0$ V is due to a small permanent dipole in the amorphous polymer, which is typical in such devices. To extract the mobility under pressure, we use formulas (1) and (2) and measure the slope of the transfer curve at sufficiently high V_G above 50 V, taking into account the pressure dependence of C . We note that the charge is completely delocalized without influence of significant traps at such high V_G . Plotted in Fig. 3(b) is the pressure dependence of the thus estimated μ . Up to 600 MPa, the mobility continuously increases with increasing pressure, which is consistent with the idea that molecular distance is diminished due to the homogeneous force that compresses the solid. On the other hand, negative pressure effect is detected above 600 MPa, which is anomalous if we project the pressure dependence only to molecular distance. We note that the effect is reversible against the repeated sweeps back and forth, as indicated in the plot showing the results of almost identical values regardless of the direction of the sweep.

Focusing on the “normal” pressure effect below 600 MPa, we discuss the observation naturally by enhanced overlap integrals between the adjacent molecules, which is translated to increase in bandwidth and decrease in effective mass in the band-transport model. Indeed, the mobility increases with decreasing temperature as plotted in Fig. 3(c), which is consistent with the assumption. The pressure coefficient for the mobility can be defined as $\Delta\mu/\mu/\Delta P$. The value estimated for the present high-mobility rubrene single crystals is as high as 0.2 GPa^{-1} , which is two orders of magnitude larger than the values for typical inorganic semiconductors such as silicon.¹¹ The difference is mainly due to the “softness” of the organic semiconductors as compared to inorganic semiconductors; typical contraction rate under pressure can differ by 50 times considering that the Young’s moduli in silicon and tetracene are 150 and 3 GPa, respectively.¹⁸

We have roughly estimated the change in principal transfer integral t_b of the highest occupied molecular orbitals (HOMOs), which is directed to the b -axis direction, using the Amsterdam density functional (ADF) program package.^{19–21} Here, we assumed the same packing geometry as the crystal structure at the ambient pressure but different molecular distance depending on the applied pressure. Taking the Young’s modulus for tetracene in the π -stacking direction for convenience, t_b can change with the factor of 0.4 GPa^{-1} , i.e., $\Delta t_b/t_b/\Delta P \sim 0.4 \text{ GPa}^{-1}$, which is linked to the pressure coefficient of the mobility because μ is inversely proportional to the effective mass and therefore can be proportional to t_b within the band-transport model. The value is indeed comparable to the experimentally deduced pressure coefficient of μ .

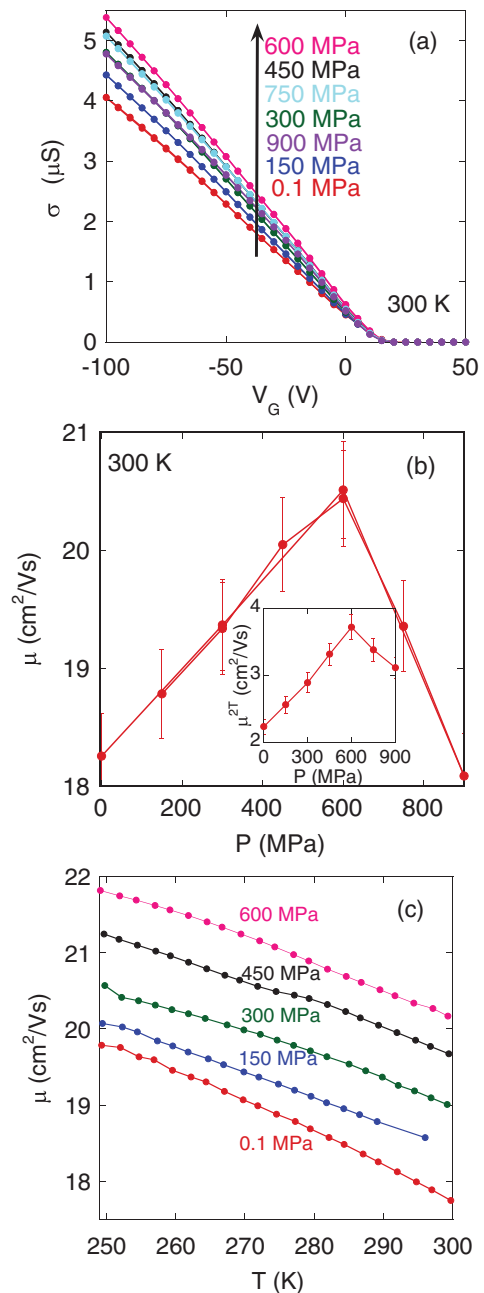


FIG. 3. (Color online) (a) Gate voltage dependence of four-terminal sheet conductivity in a rubrene single-crystal transistor under hydrostatic pressures in the range 0.1–900 MPa at 285 K. (b) Pressure dependence of carrier mobility in a rubrene single-crystal transistor. The values measured with the sweep-up and sweep-down conditions are plotted together. The same plot is shown for two-terminal mobility in the inset. (c) Temperature dependence of the mobility under hydrostatic pressures in the range 0.1–900 MPa

As compared to previously reported values in literature,^{9,10} the present $\Delta\mu/\mu/\Delta P$ is almost one order of magnitude higher. Noting that the previously obtained values were based on the two-terminal measurement including the contact resistances at source and drain electrodes, we have plotted in the inset of Fig. 3(b) the pressure-dependent mobility estimated in the same method as in the literature, i.e., $\mu^{2T} = 1/(CV_D)$.

$\partial I_D / \partial V_G \cdot L/W$. Since the value of $\Delta\mu^{2T}/\mu^{2T}/\Delta P$ is about 1.4 GPa^{-1} , much larger than the intrinsic value originating from the semiconductor channel, we conclude that the contact resistance is more sensitive to the applied pressure. The result is consistent with the results in literature.

The negative pressure coefficient above 600 MPa is anomalous if the effect is governed by molecular distance alone. However, it can be understandable assuming that relative displacement between adjacent molecules takes place in response to the pressure. It is noteworthy that rearrangement of rubrene molecules is reported preserving the face-to-face packing structure when the solid shrinks at lower temperatures.²² Though detailed structural analysis is necessary to confirm such effect with the application of pressure, it is presumable that the degree of freedom due to the specific molecular structure is relevant in the observed negative pressure coefficient.

C. Gate voltage dependence

In Fig. 4(a), room-temperature mobility is plotted as a function of V_G at 0.1 and 600 MPa. Since the subthreshold region where mobility increases drastically with $|V_G|$ is governed by charges gradually accumulated in the band-tail

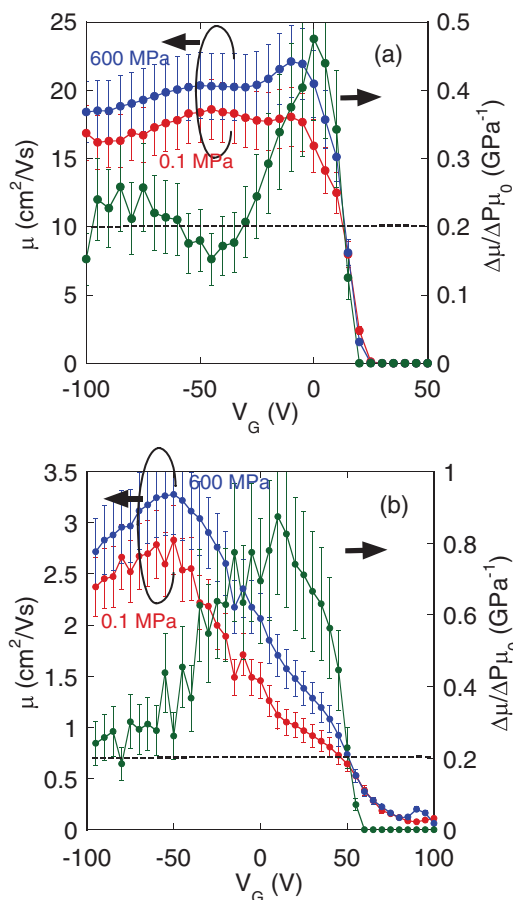


FIG. 4. (Color online) Gate voltage dependence of mobility under hydrostatic pressures of 0.1 Pa and 600 MPa for (a) high-mobility and (b) low-mobility rubrene single-crystal transistors. Pressure effect in the mobility is plotted together. Dashed lines indicate the band-transport value of the pressure coefficient.

states, the plot can highlight the pressure dependence of such slow carriers. As the pressure coefficient of $\Delta\mu/\mu/\Delta P$ is plotted together, gate voltage dependence of the pressure effect is extracted. In contrast to the high V_G region above 50 V, where the pressure coefficient is nearly constant about 0.2 GPa^{-1} , the coefficient is somewhat enhanced in the subthreshold region. In order to investigate the property in the tail states more pronouncedly, we prepared another sample with lower mobility; the sample is prepared in the same method but in a different batch, which resulted in lower average mobility possibly due to a slightly different condition on the gate dielectric surfaces. Figure 4(b) shows the same plot for a lower-mobility sample, which indeed indicates a more pronounced subthreshold feature in the transfer characteristics.

As the results of the measurement for the two samples, the the pressure coefficient of 0.2 GPa^{-1} appears to be universal for the carriers within the band, consistent with the understanding that the value is due to mass reduction intrinsic to the band-transport system. On the other hand, the enhanced pressure effect found in the subthreshold region suggests an additional mechanism when the charge in shallow trap sites is responsible. As a phenomenological model called the multiple-trap-and-release model is often used to describe the charge dynamics concerning the tail state, it is convenient to argue the observation along the context. The mobility consists of two time scales of transport time τ_{trans} and trapping time τ_{trap} , so that $\mu \propto \tau_{\text{trans}}/(\tau_{\text{trans}} + \tau_{\text{trap}})$. As we have discussed that the bandwidth is expanded by tens of % as the result of the applied pressure, this change in the energy-band diagram could affect the activation energy $\Delta(P)$ for the charge in the shallow traps. Since $\tau_{\text{trap}} (\propto \exp[-\Delta(P)/kT])$, k is the Boltzmann constant and T is the temperature, is predominant in determining μ for the charge in the shallow traps, the large $\Delta\mu/\mu/\Delta P$ in the subthreshold regime can be understood if $\Delta(P)$ decreased with increasing P as the level of the band edge moves up with the increased bandwidth as shown in the illustration. The difference in the effects between the two samples is attributed to smaller amount of the shallow-trap levels in the former higher-mobility sample.

IV. SUMMARY

The method of studying the effect of hydrostatic pressure on organic semiconductors is established employing precise measurement of both four-terminal conductivity and Hall coefficient on high-mobility rubrene single-crystal transistors with the application of gate voltages, which continuously accumulate holes from the shallow trap region to the band-edge region. When the charge density is sufficient to realize band-transport mechanism, intrinsic pressure effect of $\Delta\mu/\mu/\Delta P \sim 0.2 \text{ GPa}^{-1}$ is obtained independent of samples and further application of V_G as the result of mass reduction caused by the enhancement in intermolecular transfer integrals. In the subthreshold regime, however, the duration when charge is localized in shallow-trap levels is modified by the pressure-induced change in the band structure, giving an additional contribution to the pressure profile of the mobility. This effect indeed strongly enhances the pressure coefficient. When the applied pressure exceeds 600 MPa, an anomalous

negative pressure effect is found. The observation indicates profound effects of the hydrostatic pressure upon molecular solids caused by degrees of freedom in the relative arrangement of the adjacent molecules.

ACKNOWLEDGMENT

This work was financially supported by a Grant-in-Aid for Scientific Research (Grants No. 17069003 and No. 19360009) from MEXT, Japan.

*takeya@sanken.osaka-u.ac.jp

- ¹J. Takeya, K. Tsukagoshi, Y. Aoyagi, T. Takenobu, and Y. Iwasa, *Jpn. J. Appl. Phys.* **44**, L1393 (2005).
- ²V. Podzorov, E. Menard, J. A. Rogers, and M. E. Gershenson, *Phys. Rev. Lett.* **95**, 226601 (2005).
- ³J. Takeya, J. Kato, K. Hara, M. Yamagishi, R. Hirahara, K. Yamada, Y. Nakazawa, S. Ikehata, K. Tsukagoshi, Y. Aoyagi, T. Takenobu, and Y. Iwasa, *Phys. Rev. Lett.* **98**, 196804 (2007).
- ⁴E. Menard, V. Podzorov, S.-H. Hur, A. Gaur, M. E. Gershenson, and J. A. Rogers, *Adv. Mater. (Weinheim, Ger.)* **16**, 2097 (2004).
- ⁵C. Reese, W.-J. Chung, M.-M. Ling, M. Roberts, and Z. Bao, *Appl. Phys. Lett.* **89**, 202108 (2006).
- ⁶J. Takeya, M. Yamagishi, Y. Tominari, R. Hirahara, Y. Nakazawa, T. Nishikawa, T. Kawase, and T. Shimoda, *Appl. Phys. Lett.* **90**, 102120 (2007).
- ⁷K. Nakayama, Y. Hirose, J. Soeda, M. Yoshizumi, T. Uemura, M. Uno, W. Li, M. Jin Kang, M. Yamagishi, Y. Okada, E. Miyazaki, Y. Nakazawa, A. Nakao, K. Takimiya, and J. Takeya, *Adv. Mater.* **23**, 1626 (2011).
- ⁸H. Minemawari, T. Yamada, H. Matsui, J. Tsutsumi, S. Haas, R. Chiba, R. Kumai, and T. Hasegawa, *Nature (London)* **475**, 364 (2011).
- ⁹Z. Rang, M. I. Nathan, P. P. Ruden, V. Podzorov, M. E. Gershenson, C. R. Newman, and C. Daniel Frisbie, *Appl. Phys. Lett.* **86**, 123501 (2005).
- ¹⁰Z. Rang, M. I. Nathan, P. P. Ruden, R. Chesterfield, and C. Daniel Frisbie, *Appl. Phys. Lett.* **85**, 5760 (2004).
- ¹¹A. R. Hutson, A. Jayaraman, and A. S. Coriell, *Phys. Rev.* **155**, 786 (1967).
- ¹²V. Podzorov, V. M. Pudalov, and M. E. Gershenson, *Appl. Phys. Lett.* **82**, 1739 (2003).
- ¹³J. Takeya, C. Goldmann, S. Haas, K. P. Pernstich, B. Ketterer, and B. Batlogg, *J. Appl. Phys.* **94**, 5800 (2003).
- ¹⁴R. W. I. de Boer, T. M. Klapwijk, and A. F. Morpurgo, *Appl. Phys. Lett.* **83**, 4345 (2003).
- ¹⁵M. Yamagishi, J. Soeda, T. Uemura, Y. Okada, Y. Takatsuki, T. Nishikawa, Y. Nakazawa, I. Doi, K. Takimiya, and J. Takeya, *Phys. Rev. B* **81**, 161306(R) (2010).
- ¹⁶C. Kloc, P. G. Simpkins, T. Siegrist, and R. A. Laudise, *J. Cryst. Growth* **182**, 416 (1997).
- ¹⁷J.-F. Chang, T. Sakanoue, Y. Olivier, T. Uemura, M.-B. Dufourg-Madec, S. G. Yeates, J. Cornil, J. Takeya, A. Troisi, and H. Sirringhaus, *Phys. Rev. Lett.* **107**, 066601 (2011).
- ¹⁸M. Oehzelt, A. Eichholzer, R. Resel, G. Heimel, E. Venuti, and R. G. Della Valle, *Phys. Rev. B* **74**, 104103 (2006).
- ¹⁹ADF2008.01. SCM Theoretical Chemistry, Vrije Universiteit, Amsterdam, [<http://www.scm.com>].
- ²⁰K. Senthilkumar, F. C. Grozema, F. M. Bickelhaupt, and L. D. A. Siebbeles, *J. Chem. Phys.* **119**, 9809 (2003).
- ²¹P. Prins, K. Senthilkumar, F. C. Grozema, P. Jonkheijm, A. P. H. J. Schenning, E. W. Meijer, and L. D. A. Siebbeles, *J. Chem. Phys. B* **109**, 18267 (2005).
- ²²O. D. Jurchescu, A. Meetsma, and T. T. M. Palstra, *Acta Crystallogr. Sect. B* **62**, 330 (2006).